



Paleoclimate proxy perspective on Caribbean climate since the year 1751: Evidence of cooler temperatures and multidecadal variability

K. H. Kilbourne,¹ T. M. Quinn,^{2,3} R. Webb,⁴ T. Guilderson,^{5,6} J. Nyberg,⁷ and A. Winter⁸

Received 22 January 2008; revised 16 June 2008; accepted 27 June 2008; published 19 September 2008.

[1] Annually resolved coral $\delta^{18}\text{O}$ and Sr/Ca records from southwestern Puerto Rico are used to investigate Caribbean climate variability between 1751 and 2004 C.E. Mean surface ocean temperatures in this region have increased steadily by about 2°C since the year 1751, with Sr/Ca data indicating $2.1 \pm 0.8^\circ\text{C}$ and $\delta^{18}\text{O}$ data indicating $2.7 \pm 0.5^\circ\text{C}$. Coral geochemical records from across the tropics demonstrate that regional variability is important for understanding climate variations at centennial time scales. A strong multidecadal salinity signal in the oxygen isotope data correlates with observed multidecadal temperature variations in the Northern Hemisphere. Instrumental wind and precipitation data indicate that the most recent coral isotopic variations are caused by expansion and contraction of the steep regional salinity gradient, forced by trade wind anomalies through meridional Ekman transport. The timing of the fluctuations suggests that the multidecadal-scale wind and surface circulation anomalies might play a role in Atlantic temperature variability and meridional overturning circulation, but further work is needed to confirm this suggestion.

Citation: Kilbourne, K. H., T. M. Quinn, R. Webb, T. Guilderson, J. Nyberg, and A. Winter (2008), Paleoclimate proxy perspective on Caribbean climate since the year 1751: Evidence of cooler temperatures and multidecadal variability, *Paleoceanography*, 23, PA3220, doi:10.1029/2008PA001598.

1. Introduction

[2] Atlantic sector climate is of particular concern because of its proximity to human populations in the Americas, Europe, and Africa. North Atlantic climate is dominated by three interconnected processes, Meridional Overturning Circulation (MOC), Tropical Atlantic Variability (TAV), and the North Atlantic Oscillation (NAO)/Arctic Oscillation system [Marshall *et al.*, 2001]. Instrumental climate data indicate that the three phenomena interact on interannual to decadal time scales through connections between sea surface temperatures, atmospheric pressure, wind, and ocean circulation [Marshall *et al.*, 2001]. Paleoclimate data from the Caribbean raises the possibility of connections on even longer time scales [Schmidt *et al.*, 2004]. More climate histories from areas affected by MOC, TAV and NAO are needed to help understand the interac-

tions of these processes on multidecadal and longer time scales.

[3] Two specific problems are addressed in this paper. The first relates to the magnitude of temperature change in the tropical Atlantic on centennial time scales and the balance between regional processes and global forcings to determine tropical sea surface temperatures. It is generally thought that the climate at Earth's poles changes more drastically than the climate of the tropics in response to the same forcing because of albedo feedbacks and possibly because of atmospheric heat transport [Cai, 2005, 2006]. This concept, known as polar amplification is consistent with the current observed response of the climate system to CO_2 forcing, and with both simple and dynamically state-of-the-art climate models. Higher-latitude cooling during the Little Ice Age (~ 1400 – 1850) is thought to have been on the order of 1 – 3°C [Overpeck *et al.*, 1997, and references therein], so by the principle of polar amplification, one would expect much less change in the tropics. Some evidence indicates that the Caribbean may experience swings in temperature on the order of a few degrees [Black *et al.*, 1999, 2004, 2007; Winter *et al.*, 2000; Watanabe *et al.*, 2001; Haase-Schramm *et al.*, 2003, 2005; Goni *et al.*, 2006], much larger than expected from a tropical ocean signal. Multicentury coral records of this region are lacking and would be useful to confirm the existing proxy records from sclerosponges and sediment cores. A 2° cooling of the tropical Atlantic during recent centuries, if confirmed, indicates a strong overprint of regional climate change on the global mean. Explaining such a phenomenon could considerably further our understanding of centennial-scale

¹Environmental Policy and Science Program, McDaniel College, Westminster, Maryland, USA.

²Institute for Geophysics, Jackson School of Geosciences, University of Texas at Austin, Austin, Texas, USA.

³Department of Geological Sciences, Jackson School of Geosciences, University of Texas at Austin, Austin, Texas, USA.

⁴Earth System Research Laboratory, NOAA, Boulder, Colorado, USA.

⁵Center for Accelerator Mass Spectrometry, Lawrence Livermore National Laboratory, Livermore, California, USA.

⁶Department of Ocean Sciences and Institute of Marine Science, University of California, Santa Cruz, California, USA.

⁷Geological Survey of Sweden, Uppsala, Sweden.

⁸Department of Marine Sciences, University of Puerto Rico, Mayaguez, Puerto Rico, USA.

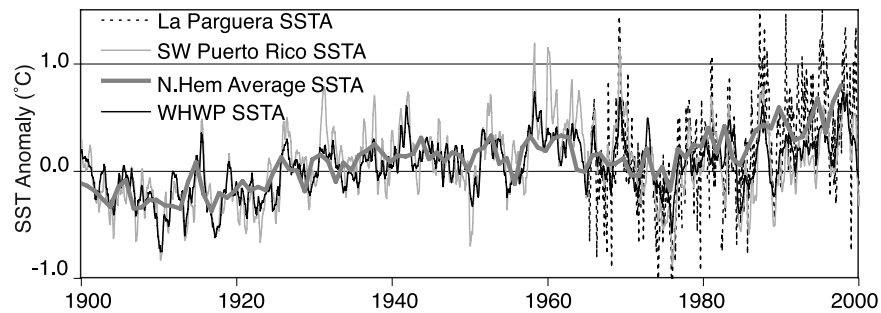


Figure 1. Sea surface temperature (SST) anomalies (SSTA) from a local record taken daily near the study site (dashed line) track larger patterns in regional and hemispheric temperature. Gridded sea surface temperature data from a $1 \times 1^\circ$ grid box including the study site (HadISST [Rayner *et al.*, 2003], centered on 17.5°N , 67.5°W) are depicted with a thin gray line. Regional average sea surface temperatures from the Western Hemisphere Warm Pool (also HadISST [Rayner *et al.*, 2003], averaged over $7\text{--}27^\circ\text{N}$ and $110\text{--}50^\circ\text{W}$) are depicted in solid black, and the Northern Hemisphere surface temperature reconstruction by Mann *et al.* [1999] using paleoclimate proxy data is wide and gray. The base period in each instance is the full record: 1966–2002 for the local SST record, 1871–2003 for the Hadley Center data, and 1902–1980 for the Mann *et al.* [1999] reconstruction. The local record has been shifted to have a similar mean over the period of overlap.

interactions of Atlantic climate processes and our understanding of regional responses to climate change.

[4] The second problem addressed by this paper involves multidecadal changes in North Atlantic sea surface temperature [Schlesinger and Ramankutty, 1994], which may be related to changes in MOC [Delworth and Mann, 2000]. It has been suggested that multidecadal-scale changes in temperature averaged over the entire Atlantic in the Northern Hemisphere may be related to precipitation patterns over North America [Enfield *et al.*, 2001] and tropical storm frequency and intensity [Landsea *et al.*, 1999; Goldenberg *et al.*, 2001]. Several modeling studies document multidecadal to centennial-scale changes in MOC that are related to similar hemispheric temperature anomalies in the Atlantic [e.g., Timmermann *et al.*, 1998; Delworth and Greatbatch, 2000; Vellinga and Wu, 2004] but instrumental data are insufficient to document such a mode in the real world [Bryden *et al.*, 2005]. Midlatitude to high-latitude tree ring records are the primary source of information documenting the persistence of a multidecadal pattern of SST anomalies over multiple centuries [Delworth and Mann, 2000; Gray *et al.*, 2004]. However, tree rings are known to have difficulty capturing multidecadal- to century-scale climate signals and replication in other proxies is needed to verify the signal [Hughes, 2002]. The multidecadal temperature anomalies in the North Atlantic have been called the Atlantic Multidecadal Oscillation [Kerr, 2000], but it remains a question if these anomalies are truly oscillatory or just red noise. If the SST anomalies are oscillatory, what is the mechanism behind the oscillation, and are the SST anomalies indeed related to MOC outside of the models?

[5] This study addresses outstanding issues of multidecadal variability and mean temperatures by producing a new 254-year coral-based paleoclimate record from southwestern Puerto Rico. Coral $\delta^{18}\text{O}$ reflects a combined signal of seawater temperature and oxygen isotopic composition during calcification, whereas coral Sr/Ca is primarily influ-

enced by seawater temperature. The oxygen isotopic composition of seawater in the tropics is strongly correlated with salinity [Fairbanks *et al.*, 1997] and is controlled by the amount of evaporation and the isotopic composition of freshwater sources. Annual coral samples are analyzed for Sr/Ca and $\delta^{18}\text{O}$ in order to produce continuous records of thermal and hydrologic variability in the northern Caribbean since 1751 C.E. The primary goal of this study is to document multidecadal- and centennial-scale climatic variability of the region and to improve our understanding of the mechanisms behind past variability by exploring this new record in the context of existing records.

2. Modern Climate Signal

[6] Puerto Rican climate is typically tropical. The local SST averages 27.9°C with a 3.2°C annual range in monthly values, derived from daily measurements between 1966 and 2002 at the field station on Magueyes Island, about 5 km from the coral coring site [Winter *et al.*, 1998]. Peak SST occurs August through October and the lowest SST is January to March. Annual SST variations from the Magueyes Island station [Winter *et al.*, 1998] correlate significantly with temperature over much larger regions (Figure 1 and Table 1). The local record tracks annual temperature from a single grid box including the study site (HadISST 1.1 [Rayner *et al.*, 2003]), the average temperature of the Western Hemisphere Warm Pool [Wang and Enfield, 2001, 2003] derived from the HadISST 1.1 data set, and a Northern Hemisphere average [Mann *et al.*, 1999].

[7] Average SSS from 1996 to 2001 at the Caribbean Time Series (CaTS) station offshore from our study site [Corredor and Morell, 2001] is 35.3 psu. The average annual cycle is 1.4 psu and the 5 years of data have a total salinity range of 2.6 psu, which occurred in a single year, illustrating the potential for substantial salinity variations in this region. The highest salinities occur March–May and the lowest salinities occur September–November. Seasonal

Table 1. Correlation Coefficients Between SST Anomalies in Figure 1^a

Correlation Coefficient (r)	La Parguera	Puerto Rico	WHWP
Northern Hemisphere	0.70	0.66	0.78
WHWP	0.79	0.89	
Puerto Rico	0.75		

^aAll correlation coefficients were calculated over the entire period of overlap between each data set pair and all are significant above the 99% confidence level.

salinity variations are controlled by the balance between the higher-salinity evaporative regime of the northern tropics and subtropics and the lower-salinity precipitation- and riverine-dominated regime to the south (Figure 2).

[8] The Caribbean Sea, including the waters just south of Puerto Rico, is influenced by continental runoff from the Orinoco and Amazon rivers year round, but the river with the most impact changes with the seasons [Froelich *et al.*, 1978; Muller-Karger *et al.*, 1989; Corredor and Morell, 2001; Hu *et al.*, 2004]. The peak effect of the Orinoco River in the northern Caribbean tends to occur in October, but the Orinoco plume commonly reaches Puerto Rico September through November [Muller-Karger *et al.*, 1989]. The peak

influence of the Orinoco River is coincident with the local peak in precipitation September–October (Magueyes Island Precipitation record distributed by Southeast Regional Climate Center <http://www.sercc.com/index.html>). Amazon river water flows into the Caribbean year round, but has the most influence in Puerto Rico June–August [Hu *et al.*, 2004]. Substantially higher salinities north of Puerto Rico indicate that the island is on the northern edge of the region strongly influenced by tropical precipitation and runoff [Corredor and Morell, 2001], and thus lies in an ideal location to detect meridional changes in this salinity gradient (Figure 2).

[9] The local $\delta^{18}\text{O}_w$ and SSS covary with the following relationship: $0.20 \pm 0.03\text{‰} \text{psu}^{-1}$, based on seawater samples collected near our study site [Watanabe *et al.*, 2001, 2002]. The $\delta^{18}\text{O}_w$ –SSS relationship is equivalent to conservative mixing between a -6.54‰ freshwater end-member and a 0.6‰ saltwater (35 psu) end-member, similar to mixing lines measured offshore of the Amazon River [Karr and Showers, 2002] and from the southern Caribbean [Fairbanks *et al.*, 1992]. The phasing of the SST and SSS annual cycles amplify the amplitude of coral $\delta^{18}\text{O}$ measurements since the seasonal increases (decreases) in tempera-

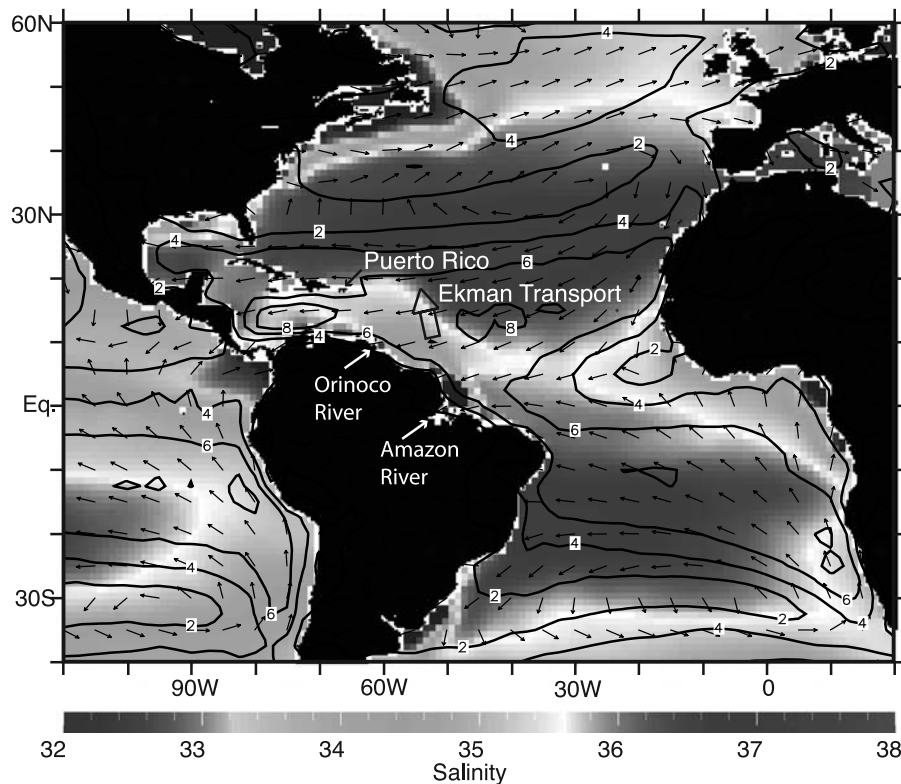


Figure 2. Mean annual surface salinity (shaded) [Antonov *et al.*, 2006] and NCEP-NCAR reanalysis surface winds [Kalnay *et al.*, 1996] with arrows indicating direction and contours indicating wind speed. Wind plot provided by NOAA/ESRL Physical Sciences Division, Boulder Colorado from their Web site at <http://www.cdc.noaa.gov>. Note that Puerto Rico lies on a steep salinity gradient. Increasing easterly winds cause a northward Ekman transport anomaly, pushing less saline water northward to be advected into the Caribbean by the westward North Equatorial Current.

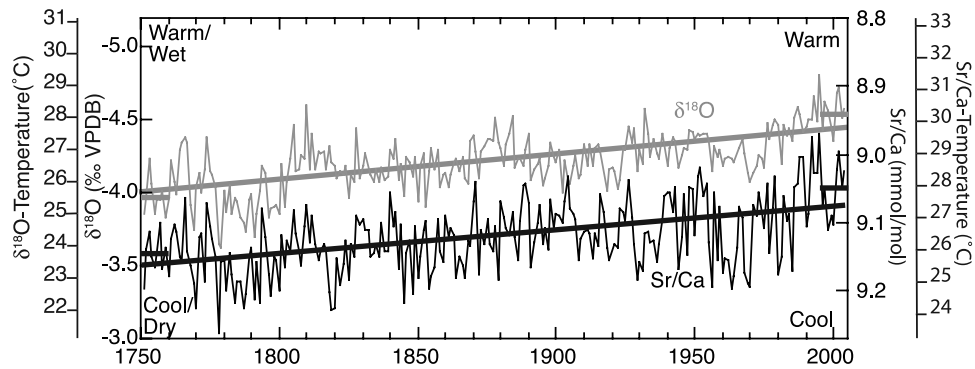


Figure 3. Annual variations in $\delta^{18}\text{O}$ (‰, gray) and Sr/Ca (mmol/mol, black) from a *Montastraea faveolata* coral from southwestern Puerto Rico. Both axes are scaled to equal 10°C using $0.047 \text{ mmol/mol } ^\circ\text{C}^{-1}$ and $0.22\text{‰ } ^\circ\text{C}^{-1}$ [Leder *et al.*, 1996; Swart *et al.*, 2002], with the 1993–2002 mean temperature (28.2°C) centered on the 1993–2002 means of the geochemical data. The 10-year averages at the beginning and end of the records are shown as gray and black bars. Long-term trends in coral Sr/Ca and $\delta^{18}\text{O}$ are highlighted and have magnitudes of 0.086 mmol/mol ($\sim 1.8^\circ\text{C}$) and 0.44‰ (2.0°C), respectively. The coral geochemical records suggest that SST has warmed $\sim 2^\circ\text{C}$ in this region since 1751.

ture coincide with decreases (increases) in salinity, both of which are recorded as a decrease (increase) in coral $\delta^{18}\text{O}$.

3. Summary of Analytical Methods

[10] A 245-cm-long core of *Montastraea faveolata* was collected at Turumote Reef (17.933°N , 67.001°W) offshore from La Parguera, Puerto Rico in August 2004. Annual subsamples, based on the annual density bands and centered on the winter season, were taken from the entire length of the core and approximately monthly subsamples were taken from the top of the coral. All of the subsamples were analyzed for Sr/Ca and $\delta^{18}\text{O}$ at the University of South Florida, College of Marine Science. Analytical precision on $\delta^{18}\text{O}$ analyses is 0.06‰ (1σ), and on Sr/Ca measurements is 0.15% or 0.013 mmol (1σ). Replicate analyses of Sr/Ca on different aliquots of the same subsample indicate that sample heterogeneity adds to the analytical error. All Sr/Ca ratios reported are averages of multiple replicates and have an error of 0.05 mmol/mol (2σ). See Appendix A for a full description of the analytical methods.

4. Geochemical Results

[11] The time series of annual coral $\delta^{18}\text{O}$ and Sr/Ca variations from 2004 to 1751 C.E. (Figure 3) are dominated by a centennial-scale trend of decreasing $\delta^{18}\text{O}$ and Sr/Ca values from the beginning of the record to the present. The magnitudes of the trends, calculated by ordinary least squares regression are 0.086 mmol/mol and 0.44‰ , equivalent to 1.8°C for Sr/Ca and 2.0°C if the $\delta^{18}\text{O}$ is interpreted completely in terms of temperature (using $0.047 \text{ mmol/mol } ^\circ\text{C}^{-1}$ and $0.22\text{‰ } ^\circ\text{C}^{-1}$ [Leder *et al.*, 1996; Swart *et al.*, 2002]). The errors on the temperature estimates are large ($\pm 2.2^\circ\text{C}$ and $\pm 1.4^\circ\text{C}$, respectively) when including the error in the regression line and the error in the original Sr/Ca-SST and $\delta^{18}\text{O}$ -SST calibrations. This is an overly pessimistic analysis because the error in the regression is largest at the high and low extremes, but we know the geochemical

values just as well at the beginning of the record as at the end. An alternate estimate of the trend comes from subtracting the mean values from the first 10 years of the records (2004–1995) and the last 10 years of the records (1760–1751). The differences between the earliest and latest decades are $0.10 \pm 0.04 \text{ mmol/mol}$ and $0.6 \pm 0.1\text{‰}$, or $2.1 \pm 0.8^\circ\text{C}$ for Sr/Ca and $2.7 \pm 0.5^\circ\text{C}$ for $\delta^{18}\text{O}$.

[12] The multidecadal mode of variance visible in plots of the $\delta^{18}\text{O}$ data (Figure 3) is confirmed by multiple spectral analysis techniques on the standard deviation normalized and linearly detrended $\delta^{18}\text{O}$ data. Significant peaks found in three different methods (Blackman-Tukey correlogram analysis (BT), multitaper method (MTM), and singular spectral analysis (SSA) with subsequent application of the maximum entropy method (MEM) using the SSA-MTM toolkit [Dettinger *et al.*, 1995; Ghil *et al.*, 2002]) are unlikely to spuriously appear above the red noise background despite the relatively short length of our record. Prefiltering the data by selecting the significant principal components from a SSA increases the signal-to-noise ratio in the time series. Subsequent spectral analysis using the MEM yields a spectrum with a tendency to have different spurious peaks than the spectra resulting from other fast Fourier transform methods [Penland *et al.*, 1991]. The dominant mode in all three spectral methods has a period of ~ 60 years per cycle, but other periods with significant variance are 4.7 years, and 2.3 years (Figure 4). The ~ 36 -year period mode found in the MTM spectrum and visible in Figure 4 is not apparent in either BT or SSA-MEM analysis and may be only a harmonic of the strong 60 year cycle.

5. Discussion

5.1. Documentation of the Climate Signal

[13] The coral faithfully records the expected climate signal in a comparison of monthly coral $\delta^{18}\text{O}$ data from 1994 to 2004, shown in Figure 5a along with the local Magueyes Island temperature record [Winter *et al.*, 1998].

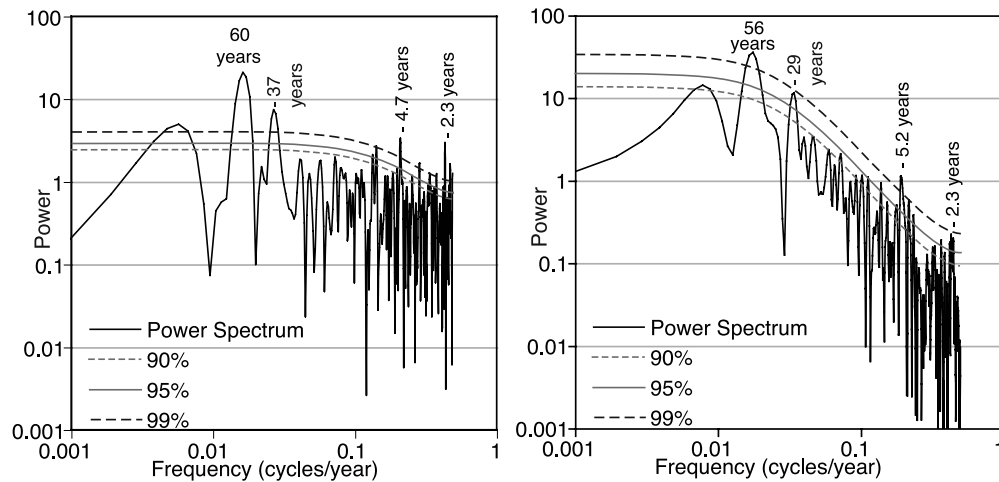


Figure 4. Power spectra (MTM) of (left) Puerto Rico coral $\delta^{18}\text{O}$ and (right) Cariaco Basin *G. bulloides* abundance time series. The Puerto Rico coral $\delta^{18}\text{O}$ shows a strong peak of spectral power above the 99% confidence level at 0.0166 cycles/a (60 year period). Only the first 249 years of the foraminiferal record were used in the analysis (1988 to 1740), and the data were resampled to annual resolution, so that the spectra were more comparable. The resulting spectrum has significant peaks at approximately the same frequencies as the coral-based spectrum.

The coral $\delta^{18}\text{O}$ data compare well with local SST and have a correlation coefficient of $r = 0.75$, which is statistically significant ($p < 0.01$) assuming only one independent data point per year in these serially correlated data. A seawater $\delta^{18}\text{O}$ reconstruction corresponds well with measured $\delta^{18}\text{O}_{\text{w}}$ data within the estimated error of the age model (± 2 months) and the propagated error of the calculations (± 0.3 ‰). The similar values of measured and calculated $\delta^{18}\text{O}_{\text{w}}$ indicates that the *Leder et al.* [1996] calibration equation is appropriate for this site.

[14] Substantial precipitation anomalies exist when the coral $\delta^{18}\text{O}$ does not mimic temperature. For example, a drought in 1997–1998 can be identified in the coral $\delta^{18}\text{O}$ data and in the local integrated precipitation anomaly in Figure 5b. Precipitation records averaged over the entire Caribbean show that the 1997–1998 drought was a regional phenomenon and was the third most severe drought since 1951, measured by departures from the 1951–2006 mean (data from *Rudolf et al.* [2005]). We tested for sensitivity to tropical storm activity by extracting 50 samples per year in 1998–1999 portion of the coral skeleton and analyzing the resultant powders for $\delta^{18}\text{O}$, looking for a strong isotopic depletion associated with the passing of Hurricane Georges, which produced 23.4 cm of rain in 3 days over the town of Lajas, just 12 km north of La Parguera (the La Parguera station did not record any data during the worst of the storm). Significant isotopic depletion during a hurricane occurs in neither the high-resolution, nor the monthly $\delta^{18}\text{O}$ data (Figure 5). The only other named tropical storm to pass within 75 km of La Parguera during 1993–2003 (Hurricane Hortense) did not produce a significant rainfall anomaly and did not register as an isotopic depletion in the coral $\delta^{18}\text{O}$. In summary, the $\delta^{18}\text{O}$ appears to be recording a combined signal of variability in SST and seawater $\delta^{18}\text{O}$, however individual short-lived tropical storm events do not substantially influence the $\delta^{18}\text{O}$ record.

[15] Monthly Sr/Ca from the same coral was too noisy to resolve the annual temperature cycle. Neither extension rate changes, nor analytical errors could explain the observed pattern of noise. Sr/Ca measurements from the top 5 cm of 4 adjacent *M. faveolata* produced similarly noisy time series, whereas Sr/Ca in an *Acropora palmata* growing on the same reef produced clearly temperature-related seasonal cycles [*Gallup et al.*, 2006]. These results indicate a biologic cause rather than an environmental cause such as changing seawater Sr/Ca. The mean value of the five *M. faveolata* Sr/Ca records produced from corals growing in this area was quite reproducible (9.12 ± 0.03 mmol/mol, 1σ), despite the variability in the data. We interpret this consistency to indicate that while we cannot rely on Sr/Ca from our coral samples to reflect seasonal variability using the monthly resolved time series, the mean over many years is a robust temperature signal. However, we utilize the Sr/Ca data cautiously because we are unable to attribute the noise to a specific cause at this time.

5.2. Long-Term Trends

[16] The long-term trends in the Puerto Rico coral $\delta^{18}\text{O}$ and Sr/Ca time series together indicate $\sim 2^\circ\text{C}$ of warming in the Caribbean since 1751 C.E. The isotopic data alone represent some combination of temperature and salinity, indicating that conditions in the 18th century were up to 2°C cooler or 2 practical salinity units (psu) less saline than today in the Northern Caribbean, assuming that the modern relationship between $\delta^{18}\text{O}_{\text{w}}$ and SSS is stationary. If Sr/Ca in this coral is dominated by temperature over the long term, despite nonclimatic noise at the higher frequencies, then the centennial trend in $\delta^{18}\text{O}$ must be due to temperature. This interpretation is consistent with the findings of previous work in the area [*Winter et al.*, 2000; *Watanabe et al.*, 2001; *Haase-Schramm et al.*, 2003]. While the Sr/Ca records from the Jamaican sclerosponge [*Haase-Schramm et al.*, 2003,

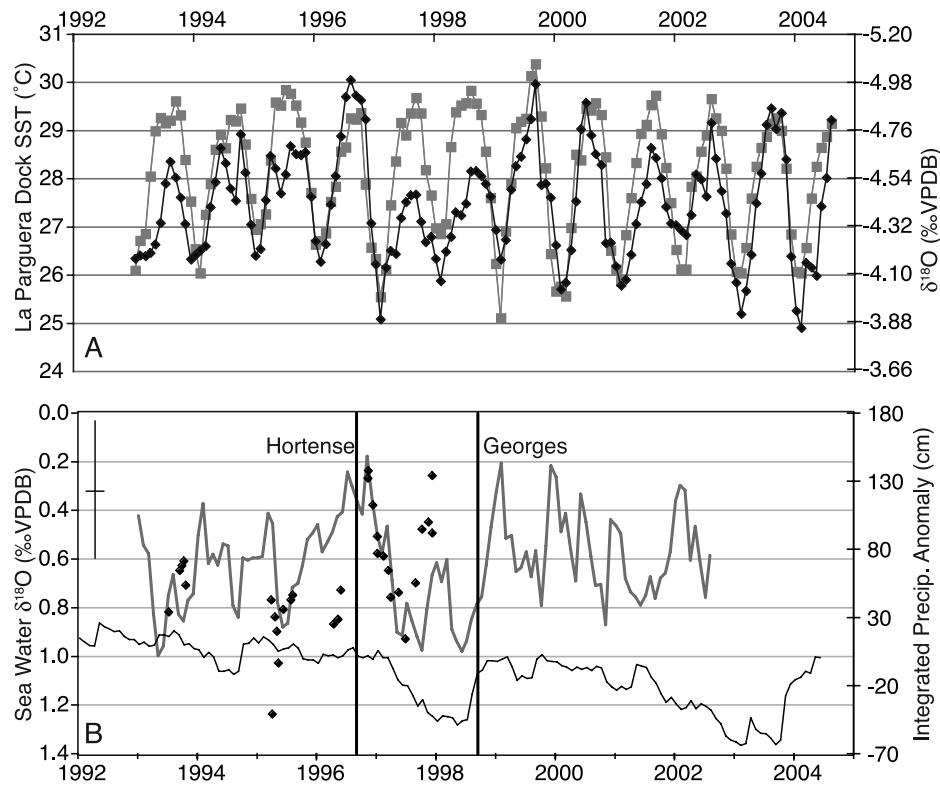


Figure 5. (a) Comparison of monthly resolved coral $\delta^{18}\text{O}$ variations (black) with a local record of monthly SST (gray), calculated from daily SST measurements at Magueyes Island. (b) Variations in seawater $\delta^{18}\text{O}$, calculated from the data in Figure 5a using the method of Gagan *et al.* [1998] and the calibration equation of Leder *et al.* [1996] (thick gray line). The error bar in the top left represents a ± 2 month estimated error in the age model (x axis) and the error propagated through the seawater $\delta^{18}\text{O}$ calculations that includes analytical error as well as calibration uncertainty (y axis). Black diamonds represent seawater $\delta^{18}\text{O}$ measurements from Watanabe *et al.* [2001]. Precipitation data are the integrated monthly rainfall anomalies from the Lajas and Magueyes Island rain gauge stations averaged together, with a base period of 1992–2004 (thin gray line, data from the Southeast Regional Climate Center <http://www.sercc.com/>). The timing of the passages of hurricanes Hortense and Georges are represented by vertical lines.

2005] and the coral from this study are ambiguous when considered individually because of their weak correlation to local instrumental temperature records, the common century-scale signal in both records, in addition to the robust coral $\delta^{18}\text{O}$ data, point to lower regional surface ocean temperature during the 1700s. While the sclerosponge record suggests that the latter 18th century was the beginning of the warming trend, our coral record is too short to confirm this suggestion.

[17] Reconstructions of cool tropical Atlantic conditions during the period known as the Little Ice Age (~ 1400 –1850) presents a climate conundrum since tropical cooling was approximately equal to high-latitude cooling at the same time [Overpeck *et al.*, 1997, and references therein], a finding that some may find at odds with the theory of polar amplification of climate change. However, spatial variability and regional climate patterns can strongly overprint the expectation from large spatial averages. To show how the tropical climate of the 18th century differed from the climate of the 20th century, we compiled the coral records with data in the 18th century from the World Data Center for

Paleoclimatology and from recently published papers. We then compared the mean for the latter 18th century (1750–1799) with the mean for the early 20th century (1900–1950) in each record (Table 2). The early 20th century was used as the reference period to avoid rapid changes at the end of the 20th century in our effort to identify anomalies during the 18th century. Our compilation indicates that areas in the western Pacific were warmer during the Little Ice Age while the Atlantic was generally cooler (Figure 6). Zonally averaged temperature in the tropics may not have been considerably different during the late 1700s, but the spatial variability was substantial. These results illustrate the significant potential for regional variations in climate change.

[18] Why might the Caribbean have been $\sim 2^{\circ}\text{C}$ cooler in the 18th century? Increased levels of Na^+ and K^+ since about 1400 in the GISP2 ice core indicate an increased storminess at high latitudes [Maasch *et al.*, 2005]. The increased storminess has been explained as an intensification of polar atmospheric circulation and more pronounced Icelandic Low, Azores High, and Siberian High [Maasch *et al.*, 2005]. This circulation pattern is similar to the positive

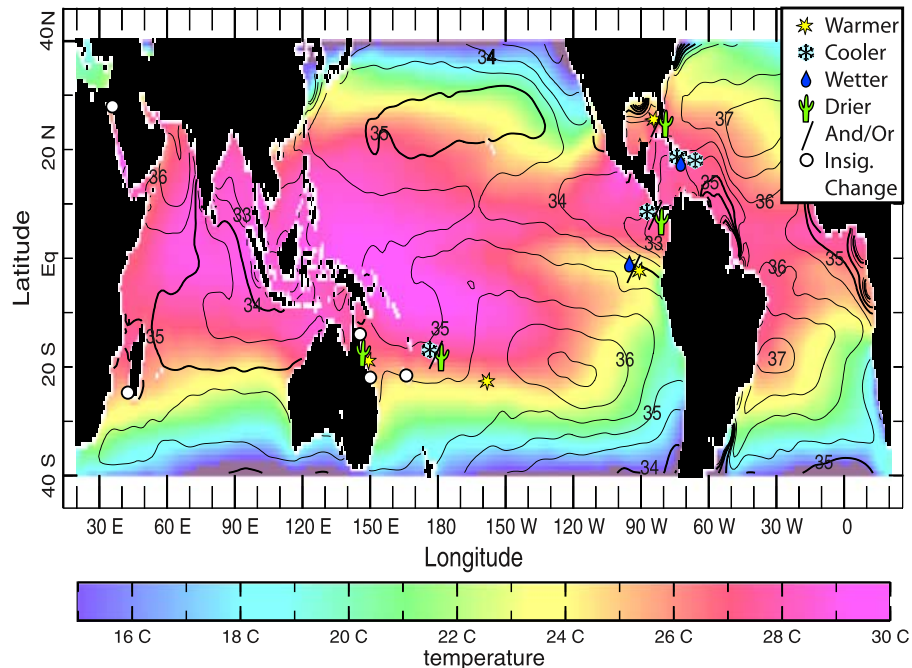


Figure 6. Mean latter 18th century tropical climate anomalies relative to the early 20th century plotted on top of mean SST (color shading) and mean SSS (contours) from *Conkright et al.* [2002]. Oxygen isotope data alone is considered ambiguous and is shown with the and/or symbol. The data show cooler conditions in the Western Hemisphere Warm Pool and generally warmer and drier conditions in the southwestern Pacific during the 1700s compared to the 1900s. All of the data are from the NOAA World Data Center for paleoclimatology, Boulder, Colorado, USA. The magnitude of the geochemical differences and the references for each data set are listed in Table 1.

phase of the Arctic Oscillation/North Atlantic Oscillation [Meeker and Mayewski, 2002]. Today, the tropical Atlantic response to a positive NAO phase is an increase in northern Hemisphere trade wind strength and cooler SST in the Northern tropics and subtropics [Marshall et al., 2001]. If the winds were consistently stronger because of a centennial-scale anomaly, then a similar cooling response is likely to have occurred. Increased trade winds during the Little Ice Age is consistent with evidence for anomalously dry conditions in the circum-Caribbean region from marine and lake sediment cores [Haug et al., 2001; Hodell et al., 2005;

Lund and Curry, 2006]. We do not see evidence of similar centennial-scale hydrologic changes in Puerto Rico, though, as the analysis of multidecadal variability described below shows, hydrologic variability at this site may be influenced by more than just evaporation and precipitation ratios.

5.3. Multidecadal Variability

5.3.1. Multidecadal Signal

[19] Coral $\delta^{18}\text{O}$ records both temperature and salinity-related seawater $\delta^{18}\text{O}$ variability so one must determine how much of the multidecadal signal is temperature, and

Table 2. Difference Between Average Geochemical Values During the Latter Half of the 18th Century and Early 20th Century^a

Site Name	Longitude	Latitude	Early Period	Late Period	Difference Sr/Ca ^b (mmol/mol)	Difference $\delta^{18}\text{O}$ ^b (‰ VPDB)	Original Reference
Abraham Reef	153.0	-22.1	1749–1799	1900–1950	–	0.09	<i>Druffel and Griffin</i> [1993]
Alina's Reef	279.8	25.4	1751–1799	1900–1950	–	0.14	<i>Swart et al.</i> [1996]
Amedee Lighthouse	166.5	-22.5	1700–1799	1900–1950	-0.033	0.08	<i>DeLong et al.</i> [2007]
Britomart Reef	146.7	-18.2	1748–1798	1903–1953	-0.026	0.15	<i>Hendy et al.</i> [2002]
Ifaty Reef	43.6	-23.2	1750–1799	1900–1950	–	-0.07	<i>Zinke et al.</i> [2004]
La Parguera	293.0	17.9	1751–1799	1900–1950	0.05	0.26	this study
Montego Bay	282.0	18.5	1747–1795	1904–1954	0.149	0.12	<i>Haase-Schramm et al.</i> [2003]
Rarotonga	200.2	-21.2	1750–1799	1900–1950	-0.090	–	<i>Linsley et al.</i> [2000]
Ras Umm Sidd	34.3	27.9	1751–1799	1900–1950	–	0.16	<i>Felis et al.</i> [2000]
Ribbon Reef	145.7	-14.7	1748–1796	1900–1950	–	0.01	<i>Worheide</i> [1998]
Savusavu Bay	179.2	-16.8	1776–1799	1900–1950	–	0.18	<i>Bagnato et al.</i> [2005]
Secas Island	278.0	8.0	1750–1798	1900–1950	–	0.18	<i>Linsley et al.</i> [1994]
Urvina Bay	268.8	-0.4	1750–1799	1900–1950	–	-0.11	<i>Dunbar et al.</i> [1994]

^aSignificant differences are highlighted in bold text. The criterion for significance was that the 2σ standard errors on the means did not overlap.

^bObtained by subtracting the average Sr/Ca and/or $\delta^{18}\text{O}$ during the late period from the average during the early period.

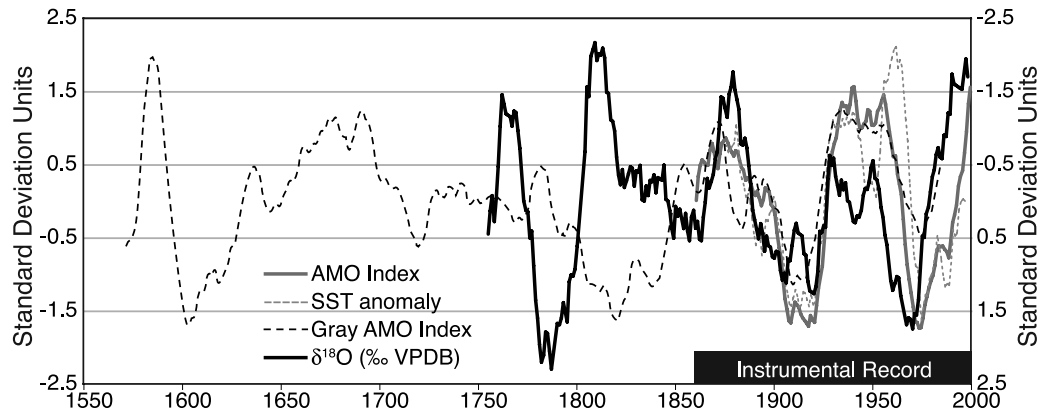


Figure 7. Multidecadal variability in Atlantic records illustrating the strong coherence between sea surface temperature anomalies (AMO index), a reconstruction from tree rings (Gray AMO index), and coral $\delta^{18}\text{O}$ (‰, VPDB) during the instrumental period, with no coherence between the two proxy data sets during the preinstrumental time. The AMO index is calculated using Kaplan SST V2 [Kaplan *et al.*, 1998], after the method of Enfield *et al.* [2001]. SST anomaly is the monthly SST anomaly for the 1° square encompassing our study area from the HadISST 1.1 data set similarly detrended and smoothed. Gray AMO index is the tree-ring-based reconstruction of the AMO from Gray *et al.* [2004], and $\delta^{18}\text{O}$ (‰VPDB) is the annual Puerto Rican coral $\delta^{18}\text{O}$ detrended and smoothed with a 10-year boxcar filter. All of the data have been centered, reduced to annual resolution if originally monthly, and normalized to one standard deviation.

how much is $\delta^{18}\text{O}$ before interpretations can be made. Relatively high correlation between $\delta^{18}\text{O}$ and Sr/Ca clearly reflects the shared temperature component of both records. The raw annual data have 43% shared variance and 26% shared variance after removing the long-term trends from both data sets. However, comparing $\delta^{18}\text{O}$ to Sr/Ca instead of directly to temperature incorporates more noise (from the Sr/Ca record) than necessary.

[20] Instrumental SST can be used to further quantify the roles of temperature and salinity in the coral $\delta^{18}\text{O}$ record. Detrended July–June annual SST anomalies from 1871 to 2002 (base period is the whole record) were smoothed with a 10-year running average and compared to similarly detrended and smoothed coral $\delta^{18}\text{O}$. The resulting curves isolate the decadal variability and are very similar to the SST and $\delta^{18}\text{O}$ curves in Figure 7, except that the curves in Figure 7 have been normalized by the standard deviation. The total range of variation in the smoothed $\delta^{18}\text{O}$ record is 0.39‰ whereas the total variation in the SST is 0.56°C . Using $0.22\text{‰}^\circ\text{C}^{-1}$ [Leder *et al.*, 1996], the SST range can account for 0.12‰ VPDB or 30% of the $\delta^{18}\text{O}$ range, leaving 0.27‰ VPDB or 70% to be accounted for by $\delta^{18}\text{O}$ and thus salinity changes. The salinity change implied in 0.27‰ VPDB is 1.3 psu assuming no change in the $\delta^{18}\text{O}$ -SSS relationship with time. Thus, the multidecadal variability is primarily a salinity signal that is of the same magnitude as the present-day seasonal salinity range.

[21] The mechanism behind the multidecadal coral isotopic variations can be investigated by examining the most recent shift. In approximately 1970, the $\delta^{18}\text{O}$ record switched from an increasing regime to a decreasing one (Figure 7). Three possible explanations are (1) evaporation decreased, (2) precipitation increased, and (3) more relatively fresh water was advected to the study site.

[22] Analysis of station-based precipitation data [Xie and Arkin, 1997; Rudolf *et al.*, 2005] and NCEP/NCAR Reanalysis surface winds [Kalnay *et al.*, 1996] suggests that precipitation and evaporation changes are unlikely explanations for the change in seawater $\delta^{18}\text{O}$. Precipitation averaged over the Caribbean shows a drying trend between 1950 and 2005, not more precipitation as needed to explain the $\delta^{18}\text{O}$ shift. Evaporation is sensitive to wind stress such that a decrease in wind velocity should decrease evaporation. NCEP/NCAR reanalysis winds strengthen in an easterly direction after 1970 around the equator and in the northern tropics. Strengthening winds should cause more evaporation and higher seawater $\delta^{18}\text{O}$. These wind data are inconsistent with the idea that evaporation caused the decreasing $\delta^{18}\text{O}$ values observed since 1970.

[23] Puerto Rico lies on a steep salinity gradient, making advection a likely candidate for changing $\delta^{18}\text{O}$ values. The Caribbean and the tropical Atlantic are considerably less saline than the surrounding ocean regions because (1) rainfall from the Intertropical Convergence Zone (ITCZ) creates a low-salinity band over the entire Atlantic basin, centered around 5°N latitude, and (2) freshwater enters the Caribbean from the Orinoco and Amazon rivers [Muller-Karger *et al.*, 1989, 1995; Hu *et al.*, 2004]. Analyses of satellite images reveals the presence of Orinoco River water in the northern Caribbean during September–November when river discharges are high [Muller-Karger *et al.*, 1989, 1995; Hu *et al.*, 2004]. This low-salinity water is transported northward, perpendicular to the prevailing surface currents by Ekman drift [Muller-Karger *et al.*, 1989]. Amazon River discharge appears to influence the Caribbean at some level constantly, but the flux of Amazon water into the Caribbean peaks around June and July, with the plume reaching Puerto Rico during June–August [Hu *et al.*, 2004].

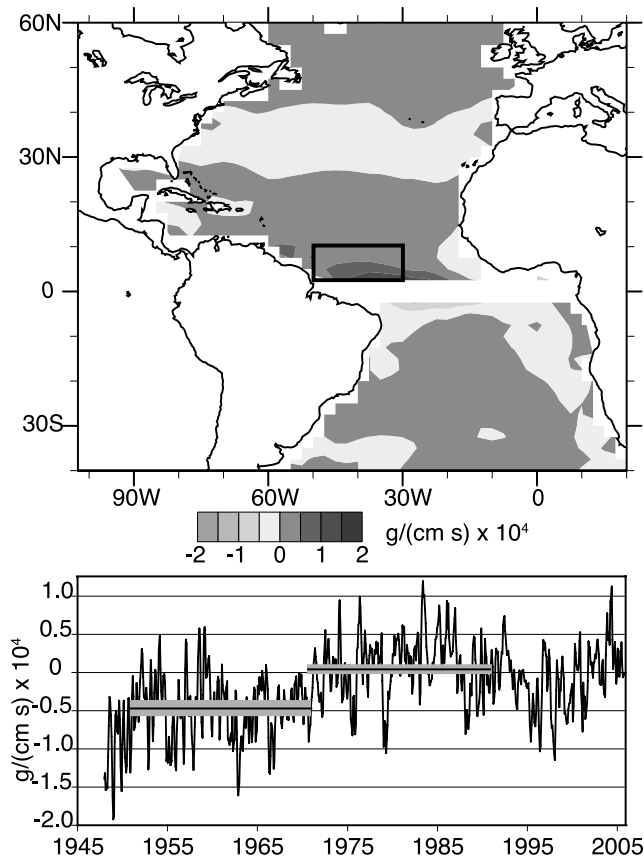


Figure 8. Ekman transport anomalies relative to 1971–2000 climatology. (top) The 1971–1990 composite minus the 1951–1970 composite. (bottom) The average over 2.5–10°N to 50–30°W, highlighted by the black rectangle in Figure 8 (top). Mean values over 1951–1970 and 1971–1990 are shown by a black bar with the 95% confidence on the mean represented by gray bars.

[24] Advection of less saline water northward can be explained by either an increase in river discharge or a stronger northward component of the surface currents bringing low-salinity water toward Puerto Rico. Precipitation over the watersheds of northern South America [Xie and Arkin, 1997; Rudolf *et al.*, 2005] has not increased post 1970, so river discharge likely has not increased either. Wind-driven surface currents are thus a more likely cause. Northward surface currents in the tropical Atlantic are primarily driven by Ekman dynamics [Mayer and Weisberg, 1993] and meridional Ekman transport is proportional to the zonal wind stress. As previously noted, the easterly wind component in the northern tropics strengthened post 1970 which would lead to an increase in the northward Ekman transport.

[25] Monthly Meridional Ekman transport anomalies ($\text{g}/(\text{cm s}) \times 10^4$) were calculated from NCEP/NCAR reanalysis monthly zonal wind data relative to 1971–2000 using the following formula:

$$V_e = \frac{\tau_u}{f}$$

where τ_u is the wind stress calculated using the zonal wind speed U (m/s) and the formula $\tau_u = \rho_a C_d U^2$. Constant values of $C_d = 1.2 \times 10^{-3}$ and $\rho_a = 1.178 \times 10^{-3} \text{ g}/\text{cm}^3$ were used. Differencing 20-year composites of the data (1951–1970 from 1971 to 1990) yields the spatial pattern of Ekman forcing resulting from the changing wind field (Figure 8). The strongest anomalies are north of the equator, in the western half of the Atlantic basin. Averaging over the region of largest anomaly highlighted by the black rectangle and smoothing to seasonal resolution yields the time series in Figure 8. The time series shows that a significant increase in the Ekman forcing occurred around 1970. The magnitude of the shift is equivalent to 20% of the seasonal range in Ekman forcing over the same region. This shift in the wind data is not believed to have been caused by a change in data assimilated into the reanalysis [Kalnay *et al.*, 1996].

[26] We propose that changes in trade wind strength and Ekman transport can explain the multidecadal $\delta^{18}\text{O}$ fluctuations in our coral record, where an increase in the average easterly wind strength in the northern equatorial region pushes equatorial water northward in the surface Ekman layer of the ocean interior (Figure 9). A decrease in average easterly wind strength will result in the opposite response with less equatorial water transported northward. Water flowing into the Caribbean from the North Equatorial Current brings the salinity characteristics of the source. If more of the lower-salinity, lower- $\delta^{18}\text{O}$ water has been pushed into the region by enhanced Ekman transport, then the inflow for the Caribbean will have lower salinity and lower $\delta^{18}\text{O}$ values.

[27] Coral $\Delta^{14}\text{C}$ from the same core as the $\delta^{18}\text{O}$ data independently indicates an increase in the amount of equatorial water reaching southwestern Puerto Rico after 1970 [Kilbourne *et al.*, 2007]. Further evidence comes from the Cariaco Basin foraminiferal abundance record of Black *et al.* [1999], representing a record of upwelling and thus trade wind strength in the southern Caribbean (Figure 9). The Cariaco record displays significant multidecadal variability that is very similar to the La Parguera coral $\delta^{18}\text{O}$ record (Figure 4). Periods of upwelling in the Cariaco basin, identified by increased *G. bulloides* abundance, tend to be associated with periods when Puerto Rico $\delta^{18}\text{O}$ decreases, indicated by gray bars in Figure 9. These changes are consistent with strengthening northeasterly trade winds causing increased upwelling along the northern coast of South America, and causing increased northward Ekman transport of low-salinity surface water. Black *et al.* [1999] evaluated the *G. bulloides* record using the entire 800-year record in a spectral analysis and did not find significant variance in the multidecadal band. The time-dependent nature of the spectral analysis results leads to the hypothesis that the mechanism causing the ~ 60 -year oscillation is sensitive to background climate and has not always been as active in the last 800 years as it has in the last 250 years.

5.3.2. Tropical and Extratropical Comparison

[28] The multidecadal variability in the Puerto Rico coral $\delta^{18}\text{O}$ record is highly correlated to hemispheric SST anomalies in the North Atlantic (Figure 7), sometimes referred to as the Atlantic Multidecadal Oscillation or AMO [Kerr, 2000]. Climate modeling studies have shown that changes

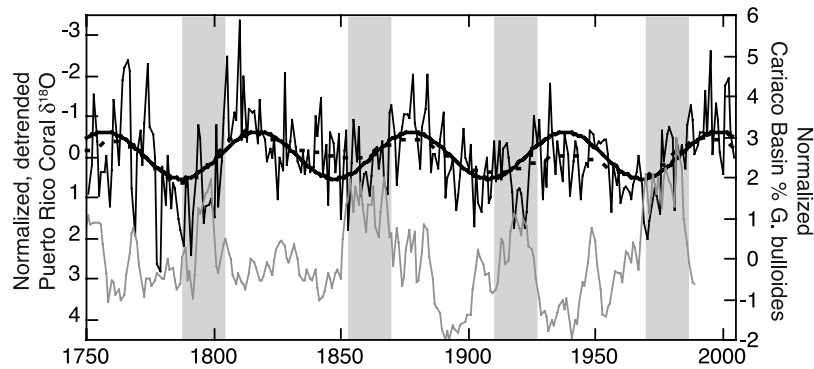


Figure 9. Puerto Rico coral $\delta^{18}\text{O}$ (thin black line) and Cariaco basin *G. bulloides* abundance (thin gray line) from Black *et al.* [1999] detrended and normalized to unit variance and zero mean. Interdecadal variability is emphasized by the reconstruction (thick black line) of the large interdecadal spectral peak (60 year period) from a Blackman-Tukey spectral analysis performed using the SSA-MTM toolkit [Dettinger *et al.*, 1995; Ghil *et al.*, 2002]. To emphasize the robust nature of this signal, the first principal component of a singular spectrum analysis (25-year window) was also used to reconstruct the time series (dotted thick line). Note that the *G. bulloides* abundance always peaks just before the Puerto Rico coral $\delta^{18}\text{O}$ reaches a minimum.

in the strength of the Atlantic meridional overturning circulation can cause hemispheric temperature anomalies similar to the observed North Atlantic SST anomalies [e.g., Delworth and Mann, 2000; Vellinga and Wood, 2002]. However, a precise mechanism for the temperature fluctuations is still a subject of study [Delworth *et al.*, 1993; Timmermann *et al.*, 1998; Delworth and Greatbatch, 2000; Delworth and Mann, 2000; Vellinga and Wu, 2004; Dijkstra *et al.*, 2006]. Despite the uncertainty, all of the proposed mechanisms for the AMO suggest that the temperature variability is related to Atlantic meridional overturning circulation and is also linked to changes in atmospheric circulation.

[29] Is the Atlantic multidecadal temperature signal merely due to ocean integration of atmospheric red noise or due to forcing by a specific oscillatory mechanism? The high correlation of the coral $\delta^{18}\text{O}$ record to North Atlantic temperature anomalies indicates that the two are related to the same processes. If this were true, then the persistence of a strong periodicity in the $\delta^{18}\text{O}$ record over the last 250 years would suggest an oscillatory mechanism rather than random noise. However, longer records are needed to demonstrate the stationarity of the apparently oscillatory $\delta^{18}\text{O}$ signal.

[30] Comparing our coral-based record of Atlantic multidecadal variability with the tree ring based AMO reconstruction of Gray *et al.* [2004] (Figure 7), both proxies track the instrumental record of North Atlantic SST anomaly well. Prior to about 1860 C.E., when the instrumental record begins, the tree ring and coral record diverge. What could cause two previously unrelated records to suddenly become coherent beginning in ~ 1860 C.E.? Some aspect of the climate system must have changed and must have affected one proxy more than the other. Wavelet analysis of both records indicates that the coral $\delta^{18}\text{O}$ record consistently has a strong 60-year period, whereas the tree ring reconstruction [Gray *et al.*, 2004] has a shift away from the 60-year period during the preinstrumental era. Since the coral record is stationary at multidecadal scales and the tree ring recon-

struction is not, we assume that the change occurred in the tree-ring-based record. The Gray *et al.* [2004] record is composed of tree ring records from the southeast United States, Fennoscandia and around the Mediterranean. All of these areas are highly sensitive to changes in the Westerlies and the position of the average storm track on interannual scales [Marshall *et al.*, 2001]. It stands to reason that they would be sensitive to such changes on even longer time scales. One possibility to explain our divergent records prior to 1860 C.E. is that centennial-scale variability could interact with the multidecadal mode enough to mask it in the extratropical records. For example, a particularly active North Atlantic polar front is hypothesized to have induced more storms in the North Atlantic region during the Little Ice Age [Maasch *et al.*, 2005], and that could have affected the tree ring records.

[31] The suggested strong connection between atmospheric forcing and ocean circulation in the tropics, and the high correlation between our $\delta^{18}\text{O}$ record and hemispheric temperature anomalies may provide insight into the connection between changes in the tropics and meridional overturning circulation. The coral $\delta^{18}\text{O}$ data show less (more) saline conditions in the tropics coinciding with warmer (cooler) North Atlantic temperatures, and thus with stronger (weaker) overturning circulation. This state of the system is very similar to the mechanism for centennial-scale overturning circulation variations in the HadCM3 model [Vellinga and Wu, 2004]. The tropical low-salinity anomalies subsequently propagate northward in the model, creating density anomalies that weaken overturning. A major difference between the model and the observational data is the cause of low salinity in the tropics. Tropical freshening in the HadCM3 model occurs because the mean ITCZ location is further north during times of strong overturning, because of the tropical wind response to the cross equatorial temperature gradient [Vellinga and Wu, 2004]. In contrast, our analysis shows that the most likely explanation is that stronger winds push more fresh equatorial water into the

Northern Hemisphere by surface Ekman drift. This mechanism provides a way to increase the transport of South Atlantic water northward (in the equatorial water) during times of strong overturning.

[32] Further work is needed to determine what sets up the wind anomalies in the first place. If the 60-year signal is periodic, then it is safe to assume that there is forcing mechanism besides stochastic noise. Internal processes involving air-sea interactions must be forcing the variance because solar forcing does not have the right periodicity and the atmospheric processes are too short lived. Possible mechanisms include low-frequency changes in the North Atlantic Oscillation and Hadley Circulation responding to North Atlantic SST [e.g., Rodwell *et al.*, 1999; Robertson *et al.*, 2000; George and Saunders, 2001; Sutton *et al.*, 2001], teleconnections with Tropical Pacific SST [e.g., Enfield and Mayer, 1997; Hoerling *et al.*, 2001], or tropical Atlantic air-sea interactions [e.g., Chang *et al.*, 1997, 2000; Wang, 2002].

6. Conclusions

[33] We interpret a 254-year record of coral $\delta^{18}\text{O}$ and Sr/Ca variations in the northern Caribbean Sea (southwestern Puerto Rico) in terms of SST and SSS variations. The long-term trends in both geochemical tracers indicate that conditions were $\sim 2^\circ\text{C}$ cooler in the 18th century compared to today. This study confirms previous studies suggesting substantial cooling in the Caribbean during the Little Ice Age [Watanabe *et al.*, 2001; Haase-Schramm *et al.*, 2003; Black *et al.*, 2007].

[34] Multidecadal variability in our data has a strong 60-year cycle that we interpret to be linked with changes in trade wind strength and the associated advection of low-salinity water from the south by Ekman transport. Temperature variations of $\sim 0.6^\circ\text{C}$ play only a minor role in the observed variability, but salinity variations are ~ 1.3 psu on these time scales. The timing of the multidecadal oscillations is consistent with a linkage to North Atlantic temperature anomalies and meridional overturning circulation. Our data indicate the persistence of a multidecadal oscillation back to at least 1750, and hint that tropical salinity variations combined with tropical surface circulation changes may be involved in the mechanism behind multidecadal variations in overturning circulation. The presence of a strong multidecadal signal since 1750 in coral and foraminiferal records from the Caribbean, along with the absence of a similarly significant peak in the full 800-year foraminiferal record indicates that the mechanism causing the multidecadal variability may be sensitive to background climate state.

[35] Further work is needed to address several issues. High-resolution paleoclimate records from the Caribbean that extend further back in time could tell us about the persistence of the cool temperatures in the 18th century, as well as addressing the question of the persistence of the multidecadal variability through centennial-scale mean state changes. The underlying mechanism behind the multidecadal variability in trade wind strength that appears to cause salinity variations is still unresolved. Possibilities include a

response to Atlantic equatorial SST gradients, to tropical Pacific forcing, or to higher-latitude processes and the state of the North Atlantic Oscillation.

Appendix A: Detailed Analytical Methods

[36] A 245-cm-long core of *Montastraea faveolata* was collected at Turrumote Reef (17.933°N , 67.001°W) offshore from La Parguera, Puerto Rico in August 2004. The coral core (04 LPT A), was cut into 5-mm-wide slabs along the primary growth axis and X-radiographed at Nova Southeastern University. The slabs were cleaned with deionized water in a sonicator and nominally annual samples of coral powder were milled from the thecal wall with a Dremel[®] tool mounted on a computer-operated drilling stage. The X-radiographs were used as a guide to ensure that one density band couplet was included in each sample. In southwestern Puerto Rico, *M. faveolata* high-density bands tend to be laid down in the early summer [Watanabe *et al.*, 2002]. The samples are thus approximately centered on January of each year. The annual coral powders were homogenized by grinding with an agate mortar and pestle until the sample reached the consistency of cornstarch (~ 10 – 20 s). The top portion of the coral slab was also milled at approximately monthly resolution with a 0.7 mm diameter bit, forming a continuous 0.7-mm-wide path. Each monthly sample consists of the material drilled in 0.6 mm of distance along the path.

[37] Counting annual density bands provided an age model for these samples. The exact position of the annual banding over core breaks was reconstructed by stacking the coral slabs together into round core sections with spacers representing the material lost in cutting the cores and with a life-size copy of the X-radiograph taped to the microdrilled slab. The two pieces of core were joined by aligning the corallites of each section, and the X-radiographs on both sides of the core break were marked exactly where they met. Once the breaks were aligned, we used the X-radiographs to count density bands multiple times. We estimate an error of ± 1 year at the bottom of the core.

[38] Sr/Ca and $\delta^{18}\text{O}$ were analyzed at the University of South Florida, College of Marine Science from aliquots of the coral powder, using a Perkin Elmer Inductively Coupled Plasma–Optical Emission Spectrometer (ICP-OES) for the elemental ratios, and a ThermoFinnigan Delta Plus XL Mass Spectrometer with a Kiel Carbonate sample preparation device for the isotopic measurements. Stable isotope measurements were obtained by reaction of 35–100 μg of aragonite with 100% phosphoric acid at 70°C and the results corrected to permil units relative to Vienna Pee Dee Belemnite (VPDB) using a calcite-based correction. Long-term precision on $\delta^{18}\text{O}$ analyses is 0.06‰ (1σ), determined by six measurements of NBS19 run daily with every set of 40 samples. Elemental data were obtained by dissolving approximately 75–200 μg of coral aragonite in enough 2% trace metal grade HNO_3 to bring the concentration of calcium to 20 ± 2 ppm (~ 1.5 – 4 ml) and analyzing the resulting solutions by ICP-OES using the method of Schrag [1999]. The precision of the Sr/Ca measurements is 0.15% or 0.013 mmol/mol (1σ , $N = 145$), determined by a

laboratory standard solution made with *Porites lutea* coral powder and run with the samples. The same precision was also obtained with a gravimetric standard solution run with the samples ($N = 97$).

[39] The elemental analysis of the annual coral samples was repeated with separate aliquots of coral powder. The average absolute difference between replicate Sr/Ca measurements was 0.03 mmol/mol and 95.5% (approximately 2σ) of the replicates were within ± 0.07 mmol/mol of each other. The difference between this replication precision and the analytical precision determined by standards run with the samples was that the replication precision includes error related to heterogeneity in the samples. The average of both

replicates was reported and therefore the data have a 2σ precision of 0.05 mmol/mol (0.07 divided by the square root of 2).

[40] **Acknowledgments.** We thank the reviewers for their constructive comments. Discussions and technical support by Jonathan Eishheid contributed to the analysis of modern precipitation data by K.H.K. Dive master Milton Carlo of the University of Puerto Rico and Captain Angel Nazario are thanked for their help with sample collection. Coral-drilling guru Fred Taylor and Peter Swart also contributed to the fieldwork. Kevin Helmle of Nova Southeastern University helped cut and X-radiograph all of the cores used in this study. Funding for this project was from National Science Foundation grant OCE-0327420 and the Elsie and William Knight Oceanographic Fellowship of the University of South Florida.

References

- Antonov, J. I., R. A. Locarini, T. P. Boyer, A. V. Mishonov, and H. E. Garcia (2006), *World Ocean Atlas 2005*, vol. 2, *Salinity*, NOAA Atlas NESDIS 62, edited by S. Levitus, 182 pp., U.S. Govt. Print. Off., Washington D. C.
- Bagnato, S., B. K. Linsley, S. S. Howe, and G. M. Wellington (2005), Coral oxygen isotope records of interdecadal climate variations in the South Pacific Convergence Zone region, *Geochim. Geophys. Geosyst.*, 6, Q06001, doi:10.1029/2004GC000879.
- Black, D. E., L. C. Peterson, J. T. Overpeck, A. Kaplan, M. N. Evans, and M. Kashgarian (1999), Eight centuries of North Atlantic ocean atmosphere variability, *Science*, 286, 1709–1713, doi:10.1126/science.286.5445.1709.
- Black, D. E., R. C. Thunell, A. Kaplan, L. C. Peterson, and E. J. Tappa (2004), A 2000-year record of Caribbean and tropical North Atlantic hydrographic variability, *Paleoceanography*, 19, PA2022, doi:10.1029/2003PA000982.
- Black, D. E., M. A. Abahazi, R. C. Thunell, A. Kaplan, E. J. Tappa, and L. C. Peterson (2007), An 8-century tropical Atlantic SST record from the Cariaco Basin: Baseline variability, twentieth-century warming, and Atlantic hurricane frequency, *Paleoceanography*, 22, PA4204, doi:10.1029/2007PA001427.
- Byden, H. L., H. R. Longworth, and S. A. Cunningham (2005), Slowing of the Atlantic meridional overturning circulation at 25°N, *Nature*, 438, 655–657, doi:10.1038/nature04385.
- Cai, M. (2005), Dynamical amplification of polar warming, *Geophys. Res. Lett.*, 32, L22710, doi:10.1029/2005GL024481.
- Cai, M. (2006), Dynamical greenhouse-plus feedback and polar warming amplification. Part 1: A dry radiative-transportive climate model, *Clim. Dyn.*, 26, 661–675, doi:10.1007/s00382-005-0104-6.
- Chang, P., L. Ji, and H. Li (1997), A decadal climate variation in the tropical Atlantic Ocean from thermodynamic air-sea interactions, *Nature*, 385, 516–518, doi:10.1038/385516a0.
- Chang, P., R. Saravanan, L. Ji, and G. C. Hegerl (2000), The effect of local sea surface temperatures on atmospheric circulation over the tropical Atlantic sector, *J. Clim.*, 13, 2195–2216, doi:10.1175/1520-0442(2000)013<2195:TEOLSS>2.0.CO;2.
- Conkright, M. E., R. A. Locarini, H. E. Garcia, T. D. O'Brien, T. P. Boyer, C. Stephens, and J. I. Antonov (2002), *World Ocean Atlas 2001: Objective Analyses, Data Statistics, and Figures*, CD-ROM Documentation, 17 pp., Natl. Oceanogr. Data Cent., Silver Spring, Md.
- Corredor, J. E., and J. M. Morell (2001), Seasonal variation of physical and biogeochemical features in eastern Caribbean Surface Water, *J. Geophys. Res.*, 106, 4517–4525, doi:10.1029/2000JC000291.
- DeLong, K. L., T. M. Quinn, and F. W. Taylor (2007), Reconstructing twentieth-century sea surface temperature variability in the southwest Pacific: A replication study using multiple coral Sr/Ca records from New Caledonia, *Paleoceanography*, 22, PA4212, doi:10.1029/2007PA001444.
- Delworth, T. L., and R. J. Greatbatch (2000), Multidecadal thermohaline circulation variability driven by atmospheric surface flux forcing, *J. Clim.*, 13, 1481–1495, doi:10.1175/1520-0442(2000)013<1481:MTCVDB>2.0.CO;2.
- Delworth, T. L., and M. E. Mann (2000), Observed and simulated multidecadal variability in the Northern Hemisphere, *Clim. Dyn.*, 16, 661–676, doi:10.1007/s003820000075.
- Delworth, T., S. Manabe, and R. J. Stouffer (1993), Interdecadal variations of the thermohaline circulation in a coupled ocean-atmosphere model, *J. Clim.*, 6, 1993–2011, doi:10.1175/1520-0442(1993)006<1993:IVOTTC>2.0.CO;2.
- Dettinger, M. D., M. Ghil, C. M. Strong, W. Weibel, and P. Yiou (1995), Software expedites singular-spectrum analysis of noisy time series, *Eos Trans. AGU*, 76, 12.
- Dijkstra, H. A., L. T. Raa, M. Schmeits, and J. Gerrits (2006), On the physics of the Atlantic multidecadal oscillation, *Ocean Dyn.*, 56, 36–50, doi:10.1007/s10236-005-0043-0.
- Druffel, E. R. M., and S. Griffin (1993), Large variations of surface ocean radiocarbon: Evidence of circulation changes in the southwestern Pacific, *J. Geophys. Res.*, 98, 20,249–20,259.
- Dunbar, R. B., G. M. Wellington, M. W. Colgan, and P. W. Glynn (1994), Eastern Pacific sea surface temperature since 1600 A. D.: The $\delta^{18}\text{O}$ record of climate variability in Galapagos corals, *Paleoceanography*, 9, 291–315, doi:10.1029/93PA03501.
- Enfield, D. B., and D. A. Mayer (1997), Tropical Atlantic sea surface temperature variability and its relation to El Niño–Southern Oscillation, *J. Geophys. Res.*, 102, 929–945, doi:10.1029/96JC03296.
- Enfield, D. B., A. M. Mestas-Núñez, and P. J. Trimble (2001), The Atlantic multidecadal oscillation and its relation to rainfall and river flows in the continental U.S., *Geophys. Res. Lett.*, 28, 2077–2080, doi:10.1029/2000GL012745.
- Fairbanks, R. G., C. D. Charles, and J. D. Wright (1992), Origin of global meltwater pulses, in *Radiocarbon After Four Decades*, edited by R. E. Taylor, pp. 473–500, Springer, Berlin.
- Fairbanks, R. G., M. N. Evans, J. L. Rubenstone, R. A. Mortlock, K. Broad, M. D. Moore, and C. D. Charles (1997), Evaluating climate indices and their geochemical proxies measured in corals, *Coral Reefs*, 16, S93–S100, doi:10.1007/s003380050245.
- Felis, T., J. Patzold, Y. Loya, M. Fine, A. H. Nawar, and G. Wefer (2000), A coral oxygen isotope record from the northern Red Sea documenting NAO, ENSO, and North Pacific teleconnections on Middle East climate variability since the year 1750, *Paleoceanography*, 15, 679–694, doi:10.1029/1999PA000477.
- Froelich, P. N., Jr., D. K. Atwood, and G. S. Giese (1978), Influence of Amazon River discharge on surface salinity and dissolved silicate concentration in the Caribbean Sea, *Deep Sea Res.*, 25, 735–744.
- Gagan, M. K., L. K. Ayliff, D. Hopley, J. A. Cali, G. E. Mortimer, J. Chappell, M. T. McCulloch, and J. M. Head (1998), Temperature and surface ocean water balance of the Mid-Holocene tropical western Pacific, *Science*, 279, 1014–1018, doi:10.1126/science.279.5353.1014.
- Gallup, C. D., D. M. Olson, R. L. Edwards, L. M. Gruhn, A. Winter, and F. W. Taylor (2006), Sr/Ca-Sea surface temperature calibration in the branching Caribbean coral *Acropora palmata*, *Geophys. Res. Lett.*, 33, L03606, doi:10.1029/2005GL024935.
- George, S. E., and M. A. Saunders (2001), North Atlantic Oscillation impact on tropical north Atlantic winter atmospheric variability, *Geophys. Res. Lett.*, 28, 1015–1018, doi:10.1029/2000GL012449.
- Ghil, M., et al. (2002), Advanced spectral methods for climatic time series, *Rev. Geophys.*, 40(1), 1003, doi:10.1029/2000RG000092.
- Goldenberg, S. B., C. W. Landsea, A. M. Mestas-Núñez, and W. M. Gray (2001), The recent increase in Atlantic hurricane activity: Causes and implications, *Science*, 293, 474–479, doi:10.1126/science.1060040.
- Goni, M. A., R. C. Thunell, M. P. Woodworth, and F. E. Muller-Karger (2006), Changes in wind-driven upwelling during the last three centuries: Interocean teleconnections, *Geophys. Res. Lett.*, 33, L15604, doi:10.1029/2006GL026415.

- Gray, S. T., L. J. Graumlich, J. L. Betancourt, and G. T. Pederson (2004), A tree-ring based reconstruction of the Atlantic Multidecadal Oscillation since 1567 AD, *Geophys. Res. Lett.*, *31*, L12205, doi:10.1029/2004GL019932.
- Haase-Schramm, A., F. Böhm, A. Eisenhauer, W.-C. Dullo, M. M. Joachimski, B. Hansen, and J. Reitner (2003), Sr/Ca ratios and oxygen isotopes from sclerosponges: Temperature history of the Caribbean mixed later and thermocline during the Little Ice Age, *Paleoceanography*, *18*(3), 1073, doi:10.1029/2002PA000830.
- Haase-Schramm, A., F. Böhm, A. Eisenhauer, D. Garbeschönberg, W.-C. Dullo, and J. Reitner (2005), Annual to interannual temperature variability in the Caribbean during the Maunder sunspot minimum, *Paleoceanography*, *20*, PA4015, doi:10.1029/2005PA001137.
- Haug, G. H., K. A. Hughen, D. M. Sigman, L. C. Peterson, and U. Röhl (2001), Southward migration of the Intertropical Convergence Zone through the Holocene, *Science*, *293*, 1304–1308, doi:10.1126/science.1059725.
- Hendy, E. J., M. K. Gagan, C. A. Alibert, M. T. McCulloch, J. M. Lough, and P. J. Isdale (2002), Abrupt decrease in tropical Pacific sea surface salinity at the end of Little Ice Age, *Science*, *295*, 1511–1514, doi:10.1126/science.1067693.
- Hodell, D. A., M. Brenner, J. H. Curtis, R. Medina-Gonzales, E. Ildefonso-Chan Can, A. Albornaz-Pat, and T. P. Guilderson (2005), Climate change on the Yucatan Peninsula during the Little Ice Age, *Quat. Res.*, *63*, 109–121, doi:10.1016/j.yqres.2004.11.004.
- Hoerling, M. P., J. W. Hurrell, and T. Xu (2001), Tropical origins for recent North Atlantic climate change, *Science*, *292*, 90–92, doi:10.1126/science.1058582.
- Hu, C., E. T. Montgomery, R. W. Schmitt, and F. E. Muller-Karger (2004), The dispersal of the Amazon and Orinoco river water in the tropical Atlantic and Caribbean Sea: Observation from space and S-PALACE floats, *Deep Sea Res., Part II*, *51*, 1151–1171.
- Hughes, M. K. (2002), Dendrochronology in climatology—the state of the art, *Dendrochronologia*, *20*, 95–116, doi:10.1078/1125-7865-00011.
- Kalnay, E., et al. (1996), The NCEP/NCAR 40-year reanalysis project, *Bull. Am. Meteorol. Soc.*, *77*, 437–471, doi:10.1175/1520-0477(1996)077<0437:TNYRP>2.0.CO;2.
- Kaplan, A., M. A. Cane, Y. Kushnir, A. Clement, M. Blumenthal, and B. Rajagopalan (1998), Analyses of global sea surface temperature 1856–1991, *J. Geophys. Res.*, *103*, 18,567–18,589, doi:10.1029/97JC01736.
- Karr, J. D., and W. J. Showers (2002), Stable oxygen and hydrogen isotopic tracers in Amazon shelf waters during Amassed, *Oceanol. Acta*, *25*, 71–78, doi:10.1016/S0399-1784(02)01183-0.
- Kerr, R. A. (2000), A North Atlantic climate pacemaker for the centuries, *Science*, *288*, 1984–1985, doi:10.1126/science.288.5473.1984.
- Kilbourne, K. H., T. M. Quinn, T. P. Guilderson, R. S. Webb, and F. W. Taylor (2007), Decadal to interannual-scale source water variations in the Caribbean Sea recorded by Puerto Rican coral radiocarbon, *Clim. Dyn.*, *29*, 51–62, doi:10.1007/s00382-007-0224-2.
- Landsea, C. W., R. A. Pielke, A. Mestas-Nunez, and J. A. Knaff (1999), Atlantic basin hurricanes: Indices of climatic changes, *Clim. Change*, *42*, 89–129, doi:10.1023/A:1005416332322.
- Leder, J. J., P. K. Swart, A. M. Szmant, and R. E. Dodge (1996), The origin of variation in the isotopic record of scleractinian corals: I. Oxygen, *Geochim. Cosmochim. Acta*, *60*, 2857–2870, doi:10.1016/0016-7037(96)00118-4.
- Linsley, B. K., R. B. Dunbar, G. M. Wellington, and D. A. Mucciarone (1994), A coral-based reconstruction of Intertropical Convergence Zone variability over Central America since 1707, *J. Geophys. Res.*, *99*, 9977–9994, doi:10.1029/94JC00360.
- Linsley, B. K., G. M. Wellington, and D. P. Schrag (2000), Decadal sea surface temperature variability in the sub-tropical South Pacific from 1726–1997 A.D., *Science*, *290*, 1145–1148, doi:10.1126/science.290.5494.1145.
- Lund, D. C., and W. Curry (2006), Florida Current surface temperature and salinity variability during the last millennium, *Paleoceanography*, *21*, PA2009, doi:10.1029/2005PA001218.
- Maasch, K. A., P. A. Mayewski, E. J. Rohling, J. C. Stager, W. Karlén, L. D. Meeker, and E. A. Meyerson (2005), A 2000-year context for modern climate change, *Geogr. Ann., Ser. A. Phys. Geogr.*, *87*, 7–15, doi:10.1111/j.0435-3676.2005.00241.x.
- Mann, M. E., R. S. Bradley, and M. K. Hughes (1999), Northern Hemisphere temperatures during the past millennium: Inferences, uncertainties, and limitations, *Geophys. Res. Lett.*, *26*, 759–762, doi:10.1029/1999GL900070.
- Marshall, J., Y. Kushnir, D. S. Battisti, P. Chang, A. Czaja, R. Dickson, J. Hurrell, M. McCartney, R. Saravanan, and M. Visbeck (2001), North Atlantic climate variability: Phenomena impacts and mechanisms, *Int. J. Climatol.*, *21*, 1863–1898, doi:10.1002/joc.693.
- Mayer, D. A., and R. H. Weisberg (1993), A description of COADS surface meteorological fields and the implied Sverdrup transports for the Atlantic Ocean from 30°S to 60°N, *J. Phys. Oceanogr.*, *23*, 2201–2221, doi:10.1175/1520-0485(1993)023<2201:ADOCSM>2.0.CO;2.
- Meeker, L. D., and P. A. Mayewski (2002), A 1400-year high-resolution record of atmospheric circulation over the North Atlantic and Asia, *Holocene*, *12*, 257–266, doi:10.1191/0959683602hl542ft.
- Muller-Karger, F. E., C. R. McClain, T. R. Fisher, W. E. Esaias, and R. Varela (1989), Pigment distribution in the Caribbean Sea: Observations from space, *Prog. Oceanogr.*, *23*, 23–64, doi:10.1016/0079-6611(89)90024-4.
- Muller-Karger, F. E., P. L. Richardson, and D. McGillicuddy (1995), On the offshore dispersal of the Amazon's plume in the North Atlantic: Comments on the paper by A. Longhurst, "Seasonal cooling and blooming in tropical oceans," *Deep Sea Res. Part I*, *42*, 2127–2137, doi:10.1016/0967-0637(95)00085-2.
- Overpeck, J. T., et al. (1997), Arctic environmental change of the last four centuries, *Science*, *278*, 1251–1256, doi:10.1126/science.278.5341.1251.
- Penland, C., M. Ghil, and K. M. Weickmann (1991), Adaptive filtering and maximum entropy spectra with application to changes in atmospheric angular momentum, *J. Geophys. Res.*, *96*, 22,659–22,671, doi:10.1029/91JD02107.
- Rayner, N. A., D. E. Parker, C. K. Horton, C. K. Folland, L. V. Alexander, D. P. Rowell, E. C. Kent, and A. Kaplan (2003), Global analyses of sea surface temperature, sea ice and night marine air temperature since the late nineteenth century, *J. Geophys. Res.*, *108*(D14), 4407, doi:10.1029/2002JD002670.
- Robertson, A. W., C. R. Mechoso, and Y.-J. Kim (2000), The influence of Atlantic sea surface temperature anomalies on the North Atlantic Oscillation, *J. Clim.*, *13*, 122–138, doi:10.1175/1520-0442(2000)013<0122:TIOASS>2.0.CO;2.
- Rodwell, M. J., D. P. Rowell, and C. K. Folland (1999), Oceanic forcing of the wintertime North Atlantic Oscillation and European climate, *Nature*, *398*, 320–323, doi:10.1038/18648.
- Rudolf, B., C. Beck, J. Brieser, and U. Schneider (2005), *Global precipitation analysis products*, pp. 1–8, Global Precip. Climatol. Cent., Dtsch. Wetterdienst, Offenbach, Germany.
- Schlesinger, M. E., and N. Ramankutty (1994), An oscillation in the global climate system of period 65–70 years, *Nature*, *367*, 723–726, doi:10.1038/367723a0.
- Schmidt, M. W., H. J. Spero, and D. W. Lea (2004), Links between salinity variation in the Caribbean and North Atlantic thermohaline circulation, *Nature*, *428*, 160–163, doi:10.1038/nature02346.
- Schrag, D. P. (1999), Rapid analysis of high-precision Sr/Ca ratios in corals and other marine carbonates, *Paleoceanography*, *14*, 97–102, doi:10.1029/1998PA900025.
- Sutton, R. T., W. A. Norton, and S. P. Jewson (2001), The North Atlantic Oscillation—What role for the ocean?, *Atmos. Sci. Lett.*, *1*, 89–100.
- Swart, P. K., R. E. Dodge, and H. J. Hudson (1996), A 240-year stable oxygen and carbon isotopic record in a coral from South Florida; implications for the prediction of precipitation in southern Florida, *Palaos*, *11*, 362–375, doi:10.2307/3515246.
- Swart, P. K., H. Elderfield, and M. J. Greaves (2002), A high-resolution calibration of Sr/Ca thermometry using the Caribbean coral *Montastraea annularis*, *Geochem. Geophys. Geosyst.*, *3*(11), 8402, doi:10.1029/2002GC000306.
- Timmermann, A., M. Latif, R. Voss, and A. Grotzner (1998), Northern Hemispheric interdecadal variability: A coupled air-sea mode, *J. Clim.*, *11*, 1906–1931.
- Vellinga, M., and R. Wood (2002), Global climatic impacts of a collapse of the Atlantic thermohaline circulation, *Clim. Change*, *54*, 251–267, doi:10.1023/A:1016168827653.
- Vellinga, M., and P. Wu (2004), Low-latitude fresh water influence on centennial variability of the Atlantic thermohaline circulation, *J. Clim.*, *17*, 4498–4511, doi:10.1175/3219.1.
- Wang, C. (2002), Atlantic climate variability and its associated atmospheric circulation cells, *J. Clim.*, *15*, 1516–1536, doi:10.1175/1520-0442(2002)015<1516:ACVAIA>2.0.CO;2.
- Wang, C., and D. B. Enfield (2001), The tropical Western Hemisphere warm pool, *Geophys. Res. Lett.*, *28*, 1635–1638, doi:10.1029/2000GL011763.
- Wang, C., and D. B. Enfield (2003), A further study of the Tropical Western Hemisphere Warm Pool, *J. Clim.*, *16*, 1476–1493.
- Watanabe, T., A. Winter, and T. Oba (2001), Seasonal changes in sea surface temperature and salinity during the little Ice Age in the Caribbean Sea deduced from Mg/Ca and ¹⁸O/¹⁶O ratios in corals, *Mar. Geol.*, *173*, 21–35, doi:10.1016/S0025-3227(00)00166-3.
- Watanabe, T., A. Winter, T. Oba, R. Anzai, and H. Ishioroshi (2002), Evaluation of the fidelity of isotope records as an environmental proxy in the coral *Montastrea*, *Coral Reefs*, *21*, 169–178.

- Winter, A., R. S. Appeldoorn, A. Bruckner, E. H. J. Williams, and C. Goenaga (1998), Sea surface temperatures and coral reef bleaching off La Parguera, Puerto Rico (northeastern Caribbean Sea), *Coral Reefs*, 17, 377–382, doi:10.1007/s003380050143.
- Winter, A., H. Ishioroshi, T. Watanabe, and T. Oba (2000), Caribbean sea surface temperatures: Two-to-three degrees cooler than present during the Little Ice Age, *Geophys. Res. Lett.*, 27, 3365–3368, doi:10.1029/2000GL011426.
- Worheide, G. (1998), The reef cave dwelling ultraconservative coralline demosponge *Astrosciera willeyana* Lister 1900 from the Indo-Pacific. Micromorphology, ultrastructure, biocalcification, isotope record, taxonomy, biogeography, phylogeny, *Facies*, 38, 1–88, doi:10.1007/BF02537358.
- Xie, P., and P. A. Arkin (1997), Global precipitation: A 17-year monthly analysis based on gauge observations, satellite estimates, and numerical model outputs, *Bull. Am. Meteorol. Soc.*, 78, 2539–2558, doi:10.1175/1520-0477(1997)078<2539:GPAYMA>2.0.CO;2.
- Zinke, J., W. C. Dullo, G. A. Heiss, and A. Eisenhauer (2004), ENSO and Indian Ocean subtropical dipole variability is recorded in a coral record off southwest Madagascar for the period 1659 to 1995, *Earth Planet. Sci. Lett.*, 228, 177–194, doi:10.1016/j.epsl.2004.09.028.
- K. H. Kilbourne, Environmental Policy and Science Program, McDaniel College, 2 College Hill, Westminster, MD 21157, USA. (kkilbourne@mcdaniel.edu)
- J. Nyberg, Geological Survey of Sweden, Box 670, SE-75128 Uppsala, Sweden.
- T. M. Quinn, Institute for Geophysics, Jackson School of Geosciences, University of Texas at Austin, 4412 Spicewood Springs Road, Austin, TX 78759, USA.
- R. Webb, Earth System Research Laboratory, NOAA, 325 Broadway, Boulder, CO 80305, USA.
- A. Winter, Department of Marine Sciences, University of Puerto Rico, P.O. Box 9013, Mayaguez, PR 00681-9013, USA.
- T. Guilderson, Center for Accelerator Mass Spectrometry, Lawrence Livermore National Laboratory, P.O. Box 808, L-397, Livermore, CA 94550, USA.